cmgh
CELLULAR AND MOLECULAR GASTROENTEROLOGY AND HEPATOLOGY

ORIGINAL RESEARCH

Prebiotic Enriched Exclusive Enteral Nutrition Suppresses Colitis via Gut Microbiome Modulation and Expansion of Anti-inflammatory T Cells in a Mouse Model of Colitis

Genelle R. Healey,[1,2] Kevin Tsai,[1] Alana Schick,[1,2] Daniel J. Lisko,[1] Laura Cook,[1] Bruce A. Vallance, PhD,[1,2,3] and Kevan Jacobson[1,3]

[1]BC Children's Hospital Research Institute, University of British Columbia, Vancouver, British Columbia, Canada; [2]Gut4Health Microbiome Core Facility, BC Children's Hospital Research Institute, University of British Columbia, Vancouver, Canada; and [3]Division of Gastroenterology, Hepatology and Nutrition, BC Children's Hospital, Vancouver, Canada

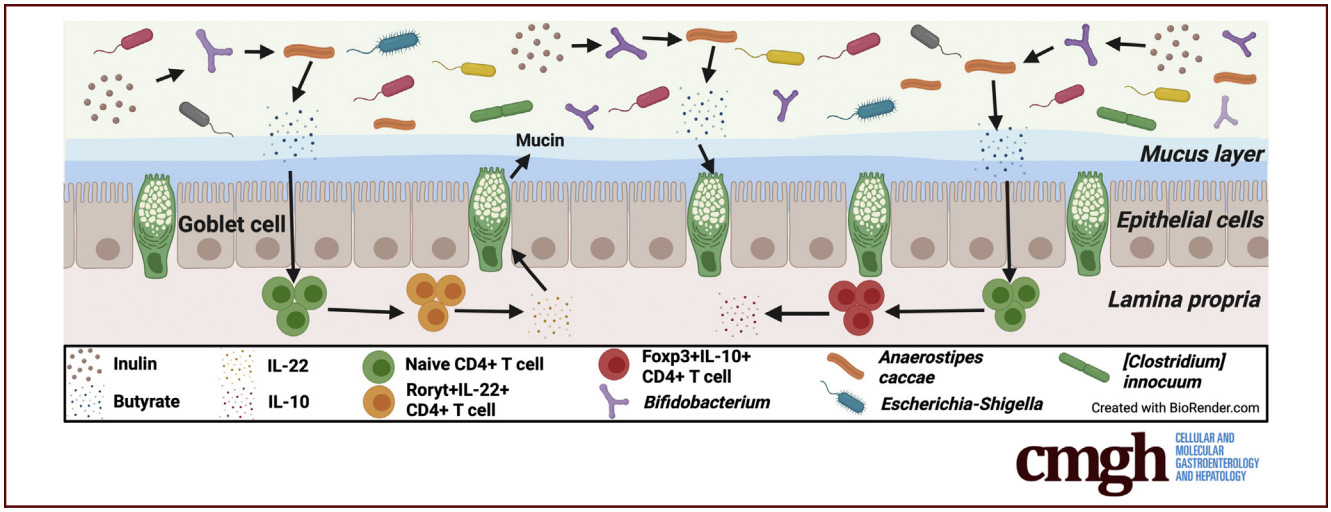

SUMMARY

We demonstrated that inulin-type fructan enriched exclusive enteral nutrition formula reduced colitis development in mice likely because of butyrate-dependent pathways that helped preserve the mucus layer and promote an anti-inflammatory intestinal environment via expansion of regulatory T cells.

BACKGROUND & AIMS: Exclusive enteral nutrition (EEN) is used to treat pediatric Crohn's disease (CD), but therapeutic benefits are variable, and EEN can lead to microbial dysbiosis. Because of reported lower efficacy EEN is not routinely used to treat pediatric ulcerative colitis (UC). Inulin-type fructans (IN) beneficially modulate the gut microbiome and promote expansion of anti-inflammatory immune cells. We hypothesized that enriching EEN with IN (EEN IN) would enhance treatment efficacy. To test this, we examined the effects of EEN IN on colitis development, the gut microbiome, and $CD4^+$ T cells using an adoptive T-cell transfer model of colitis.

METHODS: TCR-β deficient ($^{-/-}$) mice were randomized to 1 of 4 groups: (1) Control, (2) Chow, (3) EEN, and (4) EEN IN, and naive $CD4^+$ T cells were adoptively transferred into groups 2–4, after which mice were monitored for 5 weeks before experimental endpoint.

RESULTS: Mice fed EEN IN showed greater colitis protection, with colonic shortening, goblet cell, and crypt density loss reduced compared with EEN fed mice and reduced disease activity and immune cell infiltration compared with chow fed mice, and less crypt hyperplasia and higher survival compared with both groups. EEN IN mice had less deterioration in the colonic mucus layer and had increased levels of $Foxp3^+IL\text{-}10^+$ and $Ror\gamma t^+IL\text{-}22^+$ and reduced levels of $Tbet^+IFN\gamma^+$ and $Tbet^+TNF^+$ $CD4^+$ T cells. EEN IN also led to higher butyrate concentrations, *Bifidobacterium* spp. and *Anaerostipes caccae* relative abundance, and lower [*Clostridium*] *innocuum* group spp. and *Escherichia-Shigella* spp. relative abundance.

CONCLUSIONS: The EEN IN group showed reduced colitis development as compared with the chow and EEN groups. This highlights the potential benefits of EEN IN as a novel induction therapy for pediatric CD and UC patients. *(Cell Mol Gastroenterol Hepatol 2021;12:1251–1266; https://doi.org/10.1016/j.jcmgh.2021.06.011)*

Keywords: Prebiotic; Regulatory T Cells; Microbiome; Inflammatory Bowel Disease.

Inflammatory bowel disease (IBD) is characterized by chronic, relapsing inflammation of the gastrointestinal (GI) tract. The etiology of IBD is unclear, but it is thought to involve a complex interaction between genetics, the gut microbiome, and other environmental triggers that lead to an aberrant immune response. The most common forms of IBD are Crohn's disease (CD), which can affect any part of the GI tract but is primarily found in the terminal ileum and cecum; and ulcerative colitis (UC), which affects only the colon. This idiopathic, relapsing and remitting disease has no cure or universally efficacious treatment; therefore, novel therapeutic strategies to reduce the burden of disease are in high demand.[1]

Exclusive enteral nutrition (EEN), a nutritionally complete liquid diet with no food intake, is considered the gold standard treatment for inducing disease remission in newly diagnosed pediatric CD patients.[2,3] It provides comparable benefits over standard medications (ie, corticosteroids and 5-aminosalicylates agents) but also promotes mucosal healing and improved nutritional status, as well as bone health and linear growth.[4] The mechanism(s) by which EEN achieves these benefits are unknown, but changes in the gut microbiota,[5] inflammatory mediators,[6,7] and intestinal barrier function[8] are likely implicated. EEN is not routinely used in active UC patients because it is less efficacious in this patient group.[9] A reason for the lower efficacy may be related to the lack of indigestible substrates (ie, fiber or prebiotics) found in the EEN formula predominately used; therefore, by the time the EEN reaches the inflamed colon of UC patients, most of the beneficial nutrients have already been absorbed in the small bowel. Even among CD patients, the benefits of EEN are variable, with up to 30% of patients not responding clinically and up to 50% of patients not responding endoscopically to EEN.[10] EEN treatment is also often associated with a dysbiotic gut microbiota profile (ie, lower alpha diversity and *Bifidobacterium* spp. relative abundance).[11–13] We suspect the absence of prebiotics and fiber in EEN formula may be responsible for its suboptimal efficacy and outcomes in children with IBD. Hence, the addition of fiber or prebiotics to EEN formula might increase its efficacy, especially in more distal disease, and may prevent EEN associated dysbiosis.

Previous studies have demonstrated that prebiotics and fiber beneficially modulate the gut microbiome and reduce inflammation in IBD.[14–16] Inulin-type fructans (IN) appear to be particularly promising in enhancing clinical outcomes in adult IBD patients, suppressing inflammation as well as modulating the composition and function of the gut microbiome.[15,17] However, to date, no studies have investigated the therapeutic efficacy of an IN enriched EEN (EEN IN) using animal models of colitis or in IBD patients. We hypothesize that the addition of IN to EEN will lead to beneficial modulation of the gut microbiome and promote the expansion of anti-inflammatory $CD4^+$ T cells, which will lead to suppression of colitis as compared with chow and EEN fed groups. Thus, we investigated the potential anti-inflammatory and gut microbiome modulating properties of a novel EEN IN formula, as compared with fiber-free EEN and chow, using a well-established adoptive T-cell transfer model of murine colitis.

Results

Mice Fed EEN IN Were Protected From Developing Colitis. We first compared the effect of enriching EEN with IN by determining the protective effects of this diet compared with EEN alone or normal chow diet in an adoptive T-cell transfer model of colitis in TCR-β deficient ($^{-/-}$) C57BL/6 mice. As measured by disease activity score (DAS), there was significantly more colitis development in the chow group as compared with the control and EEN IN groups because more chow fed mice experienced weight loss and diarrhea. Colitis development was also lower in the EEN IN group compared with the EEN group; however, this difference did not reach significance (Figure 1*A*). The EEN fed mice had a higher body weight change at the end of the experiment when compared with all other groups (Figure 1*B*). This is likely explained by the higher calorie consumption observed in the EEN group (Table 1). Although the caloric intake in the EEN IN group was higher than in the chow and control groups, it was still lower than the EEN group likely because of the addition of fiber having a satiating effect,[18] which led to lower average amounts of formula consumed (Table 1) and subsequently less weight gain (Figure 1*B*). Moreover, all control and EEN IN mice survived until the end of the experiment; however, survival rates were only 92% and 77% in the EEN and chow groups, respectively. Several mice in these groups had to be euthanized early as they reached humane endpoint because of the development of severe colitis (Figure 1*C*). Although EEN and chow fed mice had increased spleen weights (indicating more severe colitis) compared with the control group, strikingly, spleen weights in the EEN IN group were comparable with those of the control group. The EEN IN group also had significantly lower spleen weights as compared with the chow group. Lower spleen weights in the EEN IN fed mice suggest reduced systemic inflammation particularly in comparison with the chow fed mice (Figure 1*D*). EEN IN fed mice also experienced significantly less colonic shortening compared with EEN fed mice, with colon lengths similar to control mice (Figure 1*E*).

Abbreviations used in this paper: **BCFA, branch-chain fatty acids; CD, Crohn's disease; DAS, disease activity score; EEN, exclusive enteral nutrition; EEN IN, inulin-type fructan enriched exclusive enteral nutrition; GI, gastrointestinal; GPR, G-protein coupled receptor; HDAC, histone deacetylase; IBD, inflammatory bowel disease; IL, interleukin; IN, inulin-type fructan; IP, intraperitoneal; MLN, mesenteric lymph nodes; PAS, periodic acid-Schiff; PBS, phosphate-buffered saline; PPARγ, proliferator-activated receptor gamma; SCFA, short-chain fatty acid; Tregs, regulatory T cells; UC, ulcerative colitis.**

Most current article

2352-345X
https://doi.org/10.1016/j.jcmgh.2021.06.011

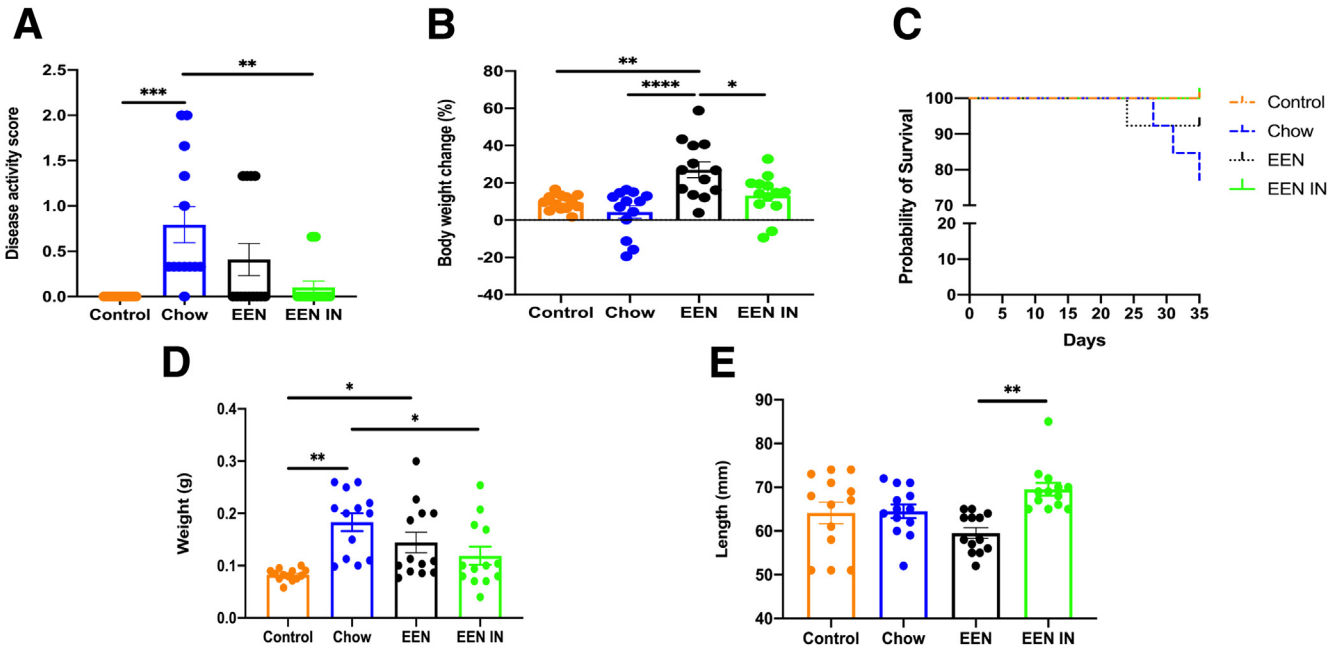

Figure 1. TCR-β deficient ($^{-/-}$) C57BL/6 mice were fed normal chow (chow), EEN, or EEN IN diet, and colitis was induced via adoptive T-cell transfer; control mice received PBS injection and were on a chow diet. (*A*) DAS, (*B*) body weight change, (*C*) survival rates, (*D*) spleen weight, and (*E*) colon length between the 4 intervention groups (n = 13 mice/group; each data point represents 1 mouse). Data shown are mean ± standard error of the mean. Statistical analysis used one-way analysis of variance. *$P < .05$, **$P < .01$, ***$P < .001$, ****$P < .0001$.

Minimal Histopathologic Changes and Loss of Mucus Layer Thickness Observed in EEN IN Fed Mice. H&E stained distal colonic sections were scored by 2 independent observers to determine whether differences in individual criteria scores were evident. The chow and EEN groups were characterized by increased inflammatory cell infiltration, goblet cell and crypt density loss, crypt hyperplasia, and submucosal inflammation compared with the control group. In contrast, only inflammatory cell infiltration was significantly elevated in the EEN IN group as compared with the control group; no other histopathologic evidence of colitis was observed (Figure 2*A* and *B*).

Mid colonic sections were stained with Alcian blue/periodic acid-Schiff (PAS) to investigate the effect each intervention had on goblet cell numbers and the mucus layer. Goblet cell numbers were significantly lower in the chow group as compared with the EEN IN group (Figure 3*A*). Although colitis in both the chow and EEN groups led to significantly thinner mucus layers, as compared with the control group, there was no significant reduction in mucus layer thickness in the EEN IN group (Figure 3*B*). Therefore, an IN enriched EEN formula helped preserve goblet cell numbers and minimized the deterioration in the mucus layer compared with chow and EEN fed mice. In addition, it appears that acidic mucins were more prevalent in the EEN and EEN IN groups (goblet cells stained blue), whereas the control and chow groups appear to have both acidic and neutral mucins (goblet cells stained a mix of magenta and purple) (Figure 3*C*).

EEN IN Results in Reduced Pro-inflammatory and Expanded Anti-inflammatory CD4$^+$ T-Cell Subsets. Next, we investigated whether there were any differences in the presence of pro-inflammatory and anti-inflammatory CD4$^+$ T-cell subsets in the spleen and mesenteric/colonic lymph nodes (MLN) between the chow, EEN, and EEN IN groups. Because the control mice were $\alpha\beta$ T-cell deficient because of the absence of function of TCR-β loci and were not adoptively transferred with naive CD4$^+$ T cells, CD4$^+$ T-cell numbers were very low compared with the other groups (0.25% versus 5.58%); therefore, these mice were not included in the CD4$^+$ T-cell subset analysis.

Chow fed mice were shown to have higher frequencies of the pro-inflammatory (Tbet$^+$IFNγ^+ and Tbet$^+$TNF$^+$) CD4$^+$ T-cell subsets in the spleen and MLN as compared with the EEN and EEN IN groups (Figure 4*B*–*E*). Although there were no significant differences in pro-inflammatory Rorγt$^+$IL-17A$^+$ CD4$^+$ T cells in the spleen and MLN between groups (Figure 4*F* and *G*), there was a significant increase in frequency of anti-inflammatory Foxp3$^+$IL-10$^+$ (regulatory T cells) and Rorγt$^+$IL-22$^+$ CD4$^+$ T cells in the spleen and MLN of mice fed EEN IN compared with mice fed a chow diet (Figure 4*H*–*K*). In addition, the frequency of splenic Rorγt$^+$IL-22$^+$ CD4$^+$ T cells was also significantly increased in the EEN IN fed mice compared with EEN fed mice (Figure 4*H*). Taken together, these data suggest that consumption of EEN IN increased the frequency of anti-colitic CD4+ T-cell subsets conferring protection against overt immune activation and colitis development.

Beneficial Modulation of the Gut Microbiome in EEN IN Fed Mice. We undertook 16s rRNA sequencing of stool samples collected before and after treatment to determine

Table 1. Nutritional Composition of Experimental Diets as well as Average Intake of Each Diet per Group

	Control/Chow	EEN	EEN IN
Diet type	Teklad TD.97184 (AIN-93G)	Ensure Plus	Ensure Plus and Orafti Synergy 1
Energy (*kcal/g* or *kcal/mL*)	3.8	1.51	1.57
Protein (%)	18.8	15.1	14.6
Fat (%)	17.2	28	27.7
Carbohydrate (%)	63.9	56.9	57.9
Fiber (%)	5	0	3
Fiber sources	Cellulose, poorly fermented	None	50:50 inulin and FOS
Average amount consumed (*g* or *mL*)	2.78 – Control; 2.49 – Chow	8.58	7.8
Average calories consumed (*kcal/day*)	10.56 – Control; 9.46 – Chow	12.96	12.24

EEN, standard exclusive enteral nutrition; EEN IN, inulin-type fructan enriched exclusive enteral nutrition; FOS, fructo-oligosaccharide.

what impact each dietary intervention had on the gut microbiota because dysbiosis (imbalance in the gut microbiota) is often associated with EEN (fiber-free) treatment. We observed a reduction in observed alpha diversity (count of unique operational taxonomy units per sample) in the chow and EEN groups from before (pre) to after (post) treatment (Figure 5*A*). We also examined whether there were changes in beta diversity (extent of change in the community composition) from before to after treatment in each group. Two distinct clusters are evident (Figure 5*B*); however, it appears that the separation in these clusters is not driven by treatment or timepoint but instead by microbiota specific cage and experiment effects (Figure 5*C*). Regardless of the cage and experiment effects, it does appear that there is a similar shift in the gut microbiota community from before to after treatment as indicated by the arrows within each treatment group pointing in a similar direction (Figure 5*D*).

Notably, several taxa specific changes in the gut microbiota were also evident within each treatment group (Figure 6*A*). Specifically, the inulin-utilizing taxa *Bifidobacterium* spp. significantly increased in the EEN IN group, whereas it significantly decreased in the EEN group after treatment (Figure 6*B* and *C*). In addition, the known butyrate-producing taxa, *Anaerostipes caccae*, increased around 100-fold in the EEN IN group but was undetectable after treatment in all other treatment groups (Figure 6*D* and *E*). Conversely, potentially pathogenic taxa such as the [*Clostridium*] *innocuum* group spp. (Figure 6*F* and *G*) and *Escherichia-Shigella* spp. (chow only) (Figure 6*H* and *I*) increased in the chow and EEN groups after treatment, whereas these bacterial taxa did not significantly change in the control and EEN IN groups.

Concentrations of certain microbial metabolites such as short-chain fatty acids (SCFAs), particularly butyrate, have also been shown to be reduced in IBD patients. Therefore, we investigated whether EEN IN could enhance butyrate production, especially because EEN IN led to a bloom in the butyrate-producer *Anaerostipes caccae*. Indeed, cecal butyrate (Figure 7*A*) production was significantly higher in the EEN IN group as compared with the chow and EEN groups. In contrast, neither cecal acetate (Figure 7*B*) nor propionate (Figure 7*C*) concentrations differed between any of the intervention groups. However, the branch-chain fatty acids (BCFAs), isobutyrate (Figure 7*D*) and isovalerate (Figure 7*E*), were found in significantly higher concentrations in the EEN group but in significantly lower concentrations after treatment in the EEN IN group, respectively. These data suggest that the addition of IN to EEN can lead to beneficial shifts in key microbial taxa, as well as a reduction in the concentrations of BCFAs and enhanced production of beneficial metabolites such as butyrate.

Discussion

In this study, we demonstrated that an EEN IN diet suppressed colitis development in an adoptive T-cell transfer model, with concomitant expansion of anti-inflammatory $CD4^+$ T cells and beneficial modulation of the gut microbiome. Specifically, consumption of an EEN IN diet led to 100% survival rate, as well as lower spleen weights, no colonic shortening, and minimal histopathologic changes in adoptive T-cell transferred mice compared with the EEN and chow groups. The EEN IN group also experienced less deterioration in the mucus layer along with higher colonic goblet cell counts. Moreover, we observed lower proportions of pro-inflammatory $CD4^+$ T cells and higher proportions of anti-inflammatory $CD4^+$ T cells in the spleen and MLN of EEN IN fed mice. Last, the gut microbiome of the EEN IN fed mice was characterized by a significant increase in relative abundance of *Bifidobacterium* spp. and *Anaerostipes caccae* and lower counts of [*Clostridium*] *innoccum* group spp. and *Escherichia-Shigella* spp. as well as higher butyrate production.

Studies have shown that consumption of IN enhances health outcomes associated with several diseases.[19,20] One key property of IN is its ability to lead to a bloom in bacterial taxa such as *Bifidobacterium* and *Lactobacillus*,[21]

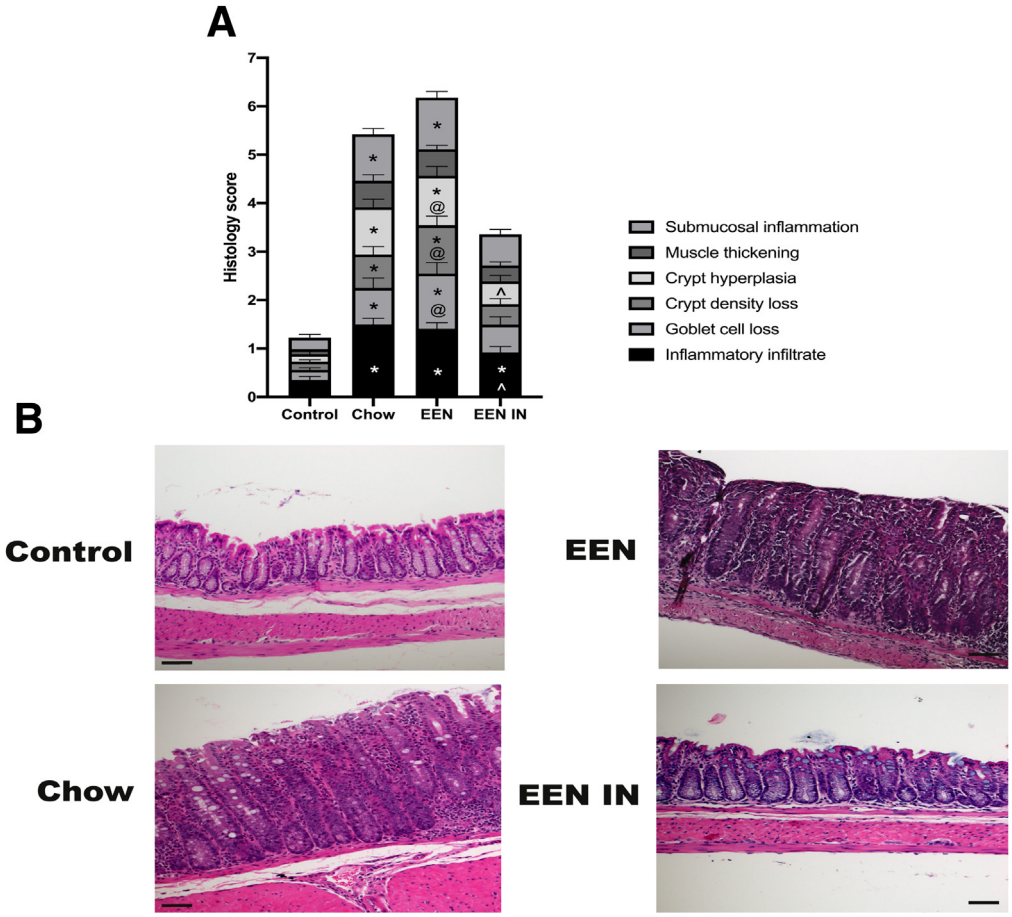

Figure 2. (*A*) Stacked bar graph showing the mean (± standard error of the mean) total histology scores as well as individual histology criteria score differences between the 4 intervention groups (n = 13 mice/group). Significant differences in individual histology criteria scores, using two-way analysis of variance, are depicted as follows: *control differs from chow, EEN, or EEN IN ($P < .05$), ^chow differs from EEN IN ($P < .05$), @ EEN differs from EEN IN ($P < .05$). (*B*) Representative images of H&E stained distal colonic tissue from the control, chow, EEN, and EEN IN groups (original magnification ×20; scale bar is 50 μm). Interpretation of these data by 2 independent observers was control, normal histopathology; chow and EEN, inflammatory infiltration, hyperplasia, submucosal inflammation, crypt density, and goblet cell loss; EEN IN, mild inflammatory infiltration.

which, because of their ability to cross feed with butyrate-producing microbes such as *Anaerostipes* spp.,[22] means IN also stimulates increased production of butyrate.[23] In fact, several of the health benefits associated with IN are thought to be related to its butyrogenic properties. Butyrate is a microbial metabolite that protects against several diseases such as colorectal cancer,[24] diabetes,[25] obesity,[25] and IBD[26] via enhanced secretion of satiety hormones,[27] maintenance of intestinal barrier function,[28] improved insulin sensitivity,[25] and regulation of immune responses.[29]

One immune cell subset known to expand in the presence of high concentrations of butyrate are regulatory T cells (Tregs).[29] Tregs are a subpopulation of $CD4^+$ T cells essential for the maintenance of immune tolerance toward self-antigens and non-self-antigens.[30] There are several Treg subsets, although the major subset is defined by expression of the master transcription factor Foxp3.[31] Although most studies on Tregs focus on their induction of xenograft tolerance, emerging evidence suggests that Tregs also induce tolerance toward resident microbiota as well as food antigens.[32,33] Despite these advancements, it is unclear whether Tregs can be induced by the microbiota and/or their metabolites through the administration of fermentable fibers such as IN. In this study we demonstrated that consumption of IN enriched EEN led to an expansion of Tregs, specifically $Foxp3^+IL\text{-}10^+$ $CD4^+$ T cells, which suggests that fermentable fibers can induce Treg differentiation likely via a pathway dependent on IN stimulated butyrate production by resident gut microbes. In addition, a key anti-inflammatory cytokine Tregs produce, interleukin (IL) 10, plays an important role in GI homeostasis, with higher production of IL10 leading to suppression of inflammation.[34] Several mechanisms have been proposed that link butyrate to the expansion of Tregs. First, butyrate acts as a ligand up-regulating peroxisome proliferator-activated receptor gamma (PPARγ) within intestinal epithelial cells, which subsequently promotes Treg differentiation and survival by regulating Foxp3.[35] The up-regulation of PPARγ can also inhibit nuclear factor kappa

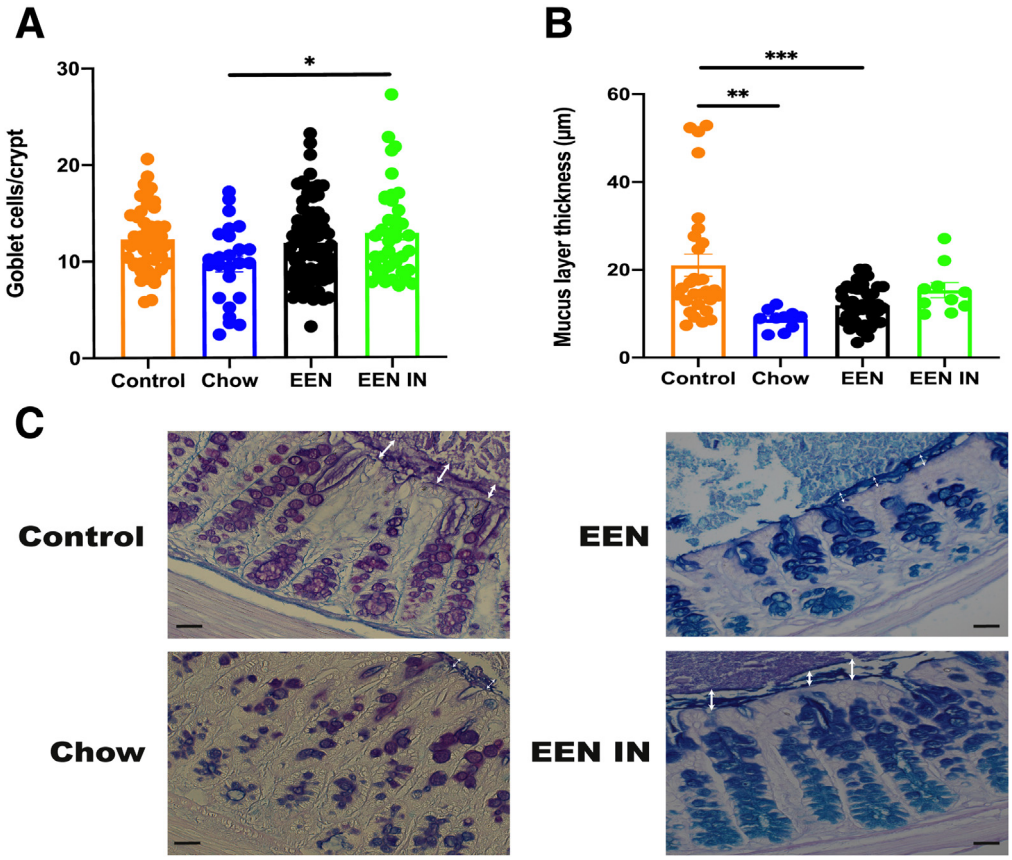

Figure 3. (*A*) Mean (± standard error of the mean) goblet cell numbers per crypt and (*B*) mucus layer thickness differences between the 4 intervention groups (n = 5–9 mice/group; each data point represents an individual measurement). (*C*) Representative images of Alcian blue/PAS stained mid colonic sections from each intervention group (original magnification ×40; scale bar is 40 μm). *White arrow* depicts the mucus layer thickness for each group. Acidic mucins stained *blue*, neutral mucins stained *magenta*, and mix of acidic and neutral mucins stained *blue/purple* within goblet cells. Statistical analysis used one-way analysis of variance. $^{*}P < .05$, $^{**}P < .01$, $^{***}P < .001$.

B, a critical pro-inflammatory transcription factor, leading to a reduction in pro-inflammatory effector T cells.[35,36] Butyrate also binds with high affinity to G-protein coupled receptors (GPR) GPR41, GPR43, and GRP109a. Butyrate bound GPRs promote antigen presenting cells (ie, dendritic cells) to differentiate toward a more tolerogenic phenotype, which subsequently induces Treg expansion and increases IL10 production.[37] Last, Foxp3 is also up-regulated via butyrate-dependent histone deacetylase (HDAC) inhibition, which potentiates the differentiation of naive T cells to Tregs.[29,38]

Increased proportions of Roryt^{+}IL-22^{+} CD4^{+} T cells were also observed in mice fed EEN IN. Similar to Tregs, the expansion of IL22 producing CD4^{+} T cells is thought to be regulated by microbiota-derived butyrate via GPR41 binding and inhibition of HDAC. CD4^{+} T-cell derived IL22 has also been shown to suppress hyperactive immune responses in the intestine[39,40] and enhance intestinal epithelial barrier function.[41] Microbiota-derived butyrate also has the capacity to regulate mucus production via an IL22-dependent mechanism.[42] This is important because an intact mucus layer provides a barrier between the underlying intestinal epithelium and the microbes and food antigens within the lumen. Deterioration or weakening of the mucus layer can lead to encroachment of luminal microbes, leading to a pro-inflammatory response by intestinal epithelial cells and underlying immune cells. In addition, butyrate, independent of IL22, is able to enhance mucosal barrier integrity directly by stimulating mucin production by goblet cells.[43] Therefore, we propose that EEN IN fed mice were protected from developing colitis via an IN-driven, butyrate-dependent expansion of anti-inflammatory and potentially mucin stimulating T-cell subsets (Foxp3^{+}IL-10^{+} and Rorγt^{+}IL-22^{+} CD4^{+} T cells).

In contrast to EEN IN fed mice, EEN and chow fed mice experienced colitis ranging from mild/moderate to severe. The EEN and chow groups both lacked fermentable fiber substrates, which may at least partially explain the suboptimal outcomes observed in these groups as compared with the EEN IN group. Previous research has shown that chronic or intermittent reductions in dietary fiber cause the gut microbiota to use endogenous fermentable substrates, such as mucin glycoproteins within the intestinal mucus layer, as an energy source. A fiber-devoid diet subsequently leads to a shift in the gut microbiota from fiber-utilizing to mucus-eroding taxa. This leads to mucus layer deterioration and intestinal barrier dysfunction, which promotes intestinal inflammation.[44,45] Dietary fiber deprivation also leads to a reduction in butyrate production,[46] impairing the beneficial immunomodulatory properties associated with this microbial metabolite (as outlined above). Therefore, the lack of available fermentable fiber in the EEN and chow diets likely promoted colitis development via deterioration of the mucus layer,

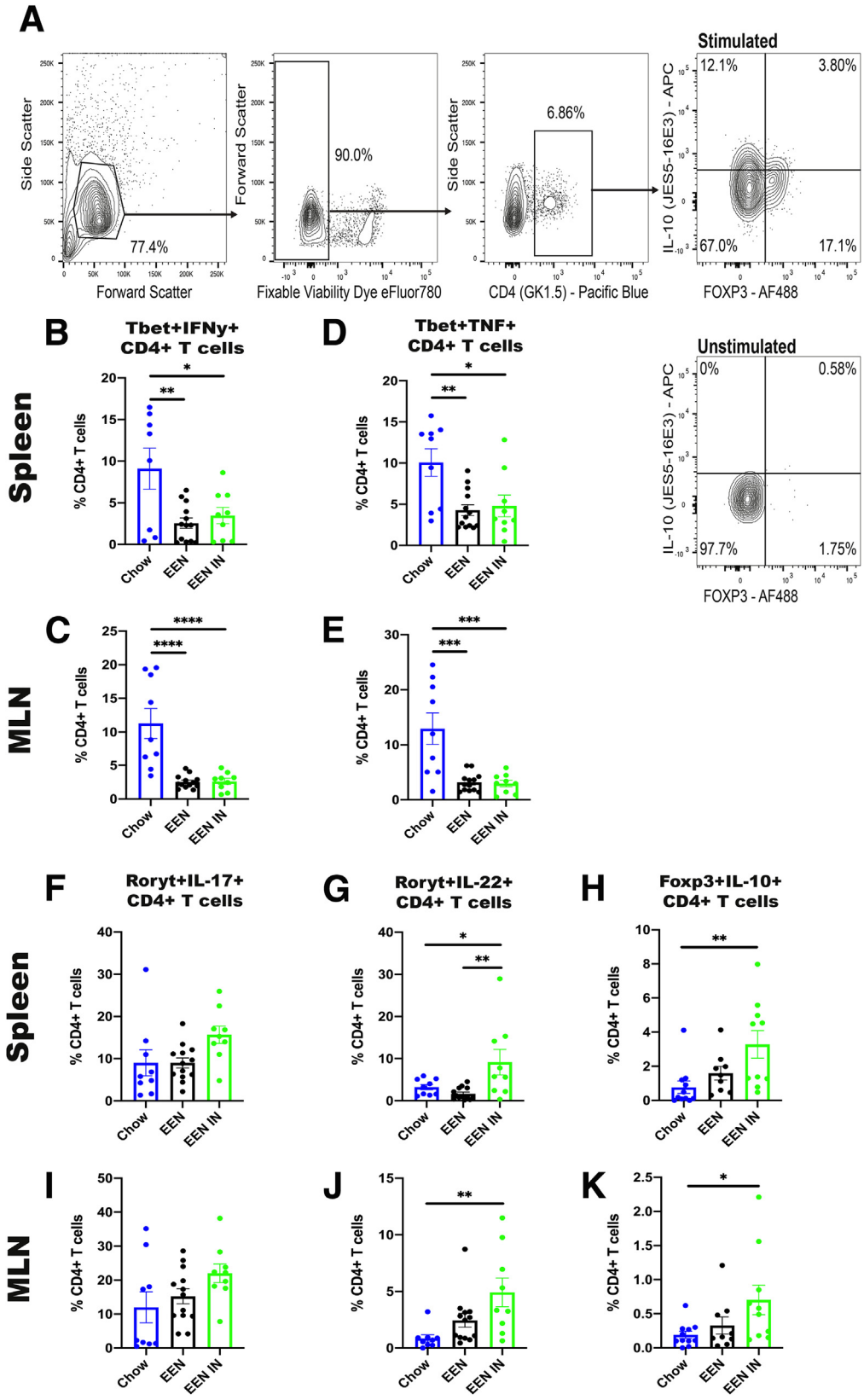

Figure 4. (*A*) Representative gating strategy for enumeration of Foxp3$^+$IL-10$^+$ CD4$^+$ T cells. Proportions of Tbet$^+$IFNγ^+ ([*B*] spleen and [*C*] MLN), Tbet$^+$TNF$^+$ ([*D*] spleen and [*E*] MLN), Rorγt$^+$IL-17A$^+$ ([*F*] spleen and [*G*] MLN), Rorγt$^+$IL-22$^+$ ([*H*] spleen and [*I*] MLN), and Foxp3$^+$IL-10$^+$ ([*J*] spleen and [*K*] MLN) CD4$^+$ T cells in mice from the chow, EEN, and EEN IN groups (n = 8–13 mice per group; each data point represents 1 mouse). Statistical analysis used one-way analysis of variance. **P* < .05, ***P* < .01, ****P* < .001, *****P* < .0001.

alterations in gut microbiota composition, reduced butyrate production, and an imbalance in pro- vs anti-inflammatory CD4$^+$ T-cell subsets.

EEN and chow feeding led to a dysbiotic gut microbiota profile characterized by reduced alpha diversity, a bloom in the potentially pathogenic microbes [*Clostridium*]

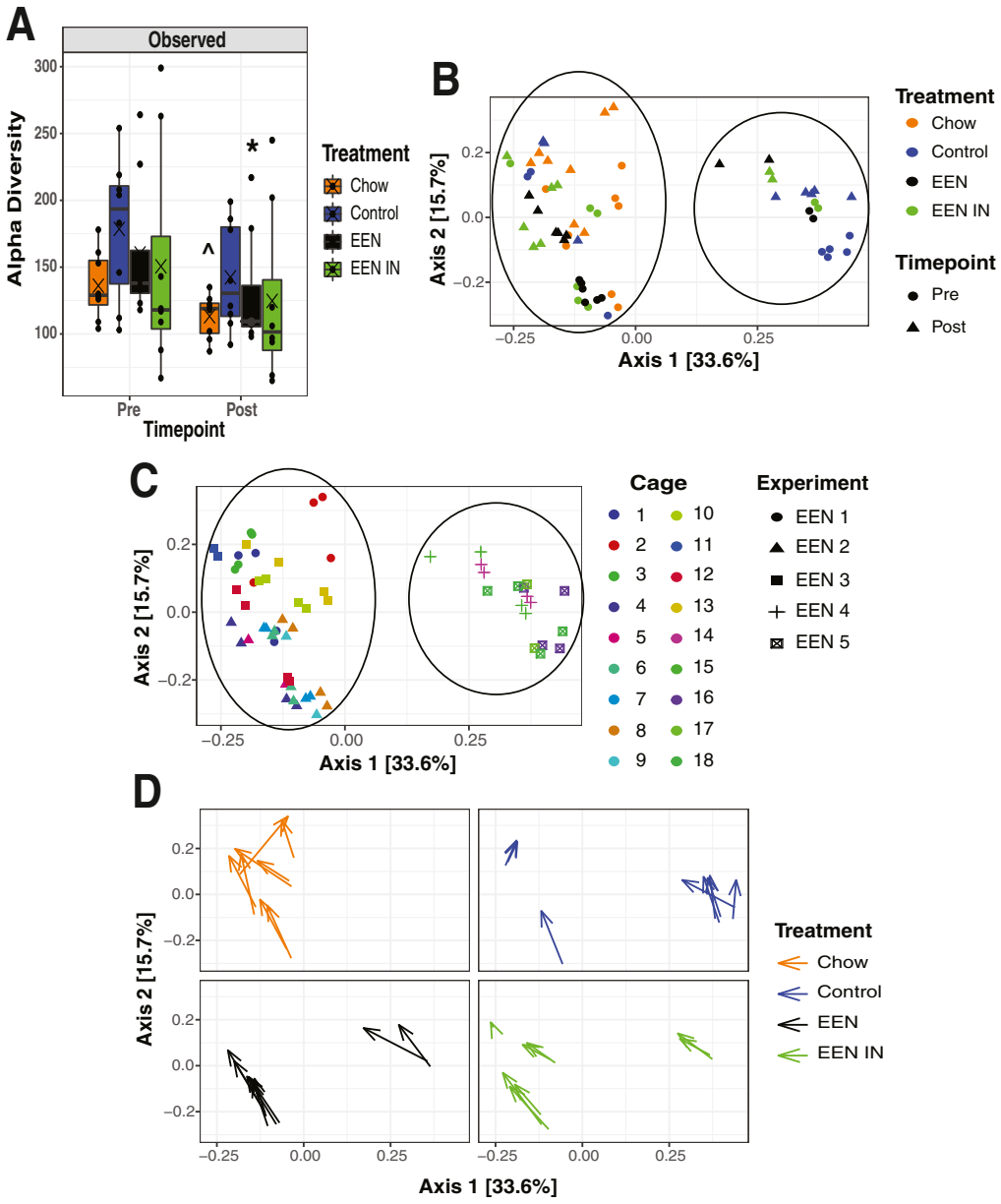

Figure 5. (*A*) Change in observed alpha diversity (within sample gut microbiota differences) between treatment groups before (pre) and after (post) treatment. (*B*) Principal co-ordinate analysis (PCoA) plot showing differences in beta diversity (between sample gut microbiota differences) between treatment groups before and after T-cell transfer and dietary intervention. *Circles* indicate the 2 distinct clusters. (*C*) PCoA plot showing differences in beta diversity between experiments and cages the mice were housed in. *Circles* indicate the 2 distinct clusters. (*D*) Individual PCoA plots for each treatment group with *arrows* depicting the change in beta diversity before and after treatment for each sample (n = 8 mice/group; each data point represents 1 mouse). Statistical analysis used Wilcoxon rank-sum test. ^$P < .06$, *$P < .05$.

innocuum group spp. and *Escherichia-Shigella* spp. (chow only), and less beneficial microbes such as *Bifidobacterium* spp. and *Anaerostipes caccae*. Maintaining a more diverse gut microbiota composition is generally considered beneficial to health, with lower alpha diversity being associated with several disease states such as irritable bowel syndrome,[47] obesity,[48] and IBD.[49] Previous studies have demonstrated that EEN interventions in CD patients lead to rapid reductions in microbial diversity,[50] which aligns with what we observed in mice fed EEN. EEN and chow fed mice also experienced a bloom in bacterial taxa known to cause bacteremia[51] and recurrent diarrhea,[52] be in higher abundances in IBD patients,[12] and/or are associated with non-sustained remission once EEN is discontinued.[13] The increase in potentially pathogenic bacteria paralleled a significant reduction in bacteria with known anti-inflammatory properties such as *Bifidobacterium* spp.,[53] as well as butyrate-producing bacteria (ie, *Anaerostipes caccae*)[22] in the EEN and chow groups. In addition, both the chow and EEN groups had similar levels of the SCFAs analyzed, and the chow and EEN groups had lower butyrate concentrations compared with the EEN IN group. Moreover, the chow group had higher levels of the BCFA isovalerate, and the EEN group had higher levels of both isovalerate and isobutyrate. BCFAs, such as isovalerate and isobutyrate, are indicative of proteolytic fermentation.[54] Because of the lack of fiber in these diets it is possible that the shifts in the gut microbiome led to higher rates of fermentation of amino acids, promoting BCFA production. Little is known about the physiological role BCFAs play,

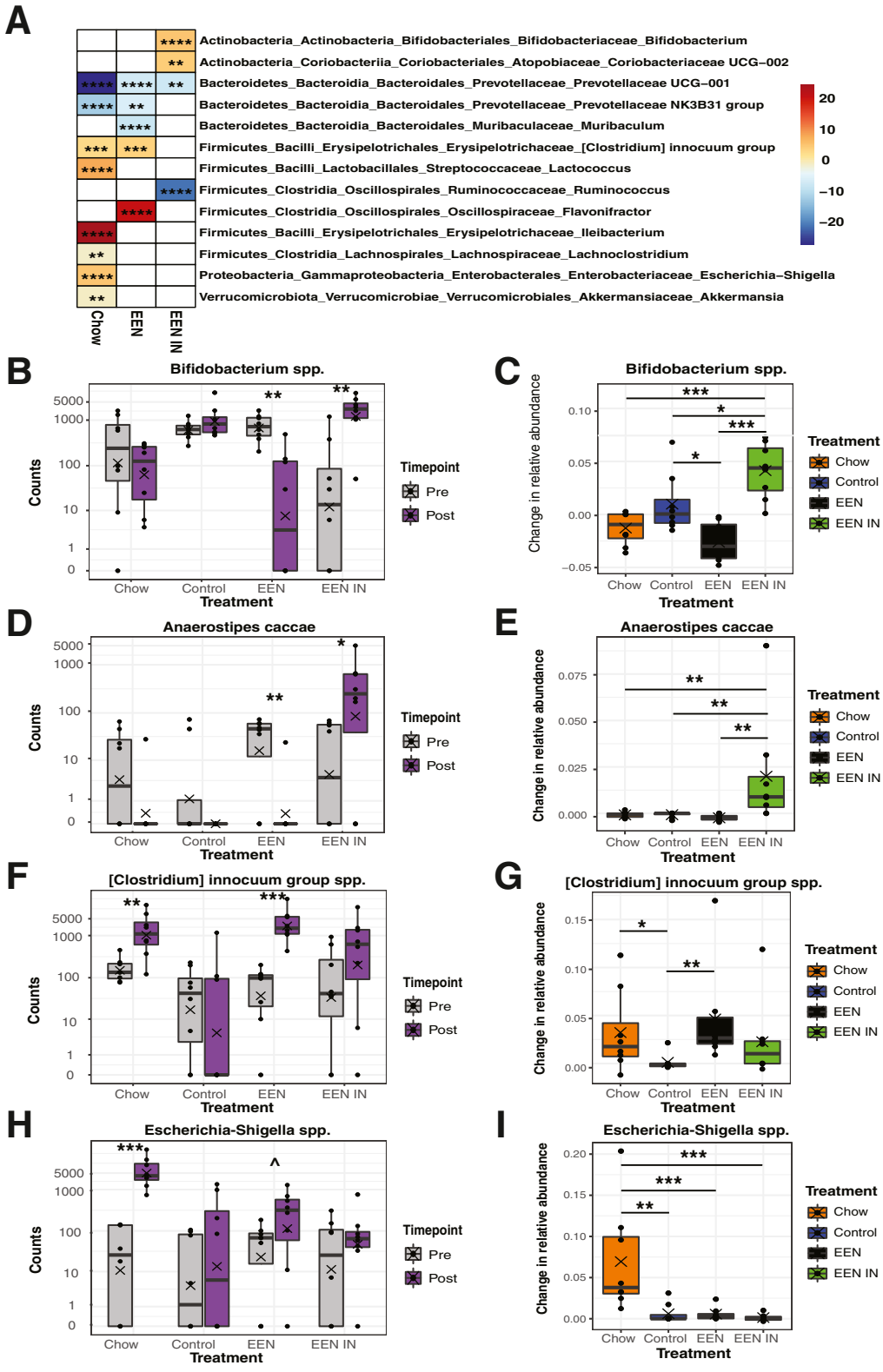

Figure 6. (*A*) Differential abundance plot with color scale representing (log2) fold change in each significant genus per treatment group between pre- and post-treatment (*red*, increased relative abundance; *blue*, decrease relative abundance). Blank cells were not statistically significant. Changes in total counts and relative abundance within and between each treatment group, respectively, for *Bifidobacterium* spp. (*B* and *C*), *Anaerostipes caccae* (*D* and *E*), [*Clostridium*] *innocuum* group spp. (*F* and *G*), and *Escherichia-Shigella* spp. (*H* and *I*) (n = 8 mice/group; each data point represents 1 mouse). Statistical analysis used Wald test and Kruskall-Wallis test. ^$P < .06$, *$P < .05$, **$P < .01$, ***$P < .001$, ****$P < .0001$.

but some studies suggest that increased protein fermentation and subsequent BCFA production may have detrimental effects on health.[54,55] Taken together, it appears that a lack of fiber in the chow and EEN diets led to thinning of the protective mucus layer and a shift toward a more dysbiotic gut microbiome profile, which resulted in the proliferation of pro-inflammatory effectors $CD4^+$ T cells and subsequent development of colitis.

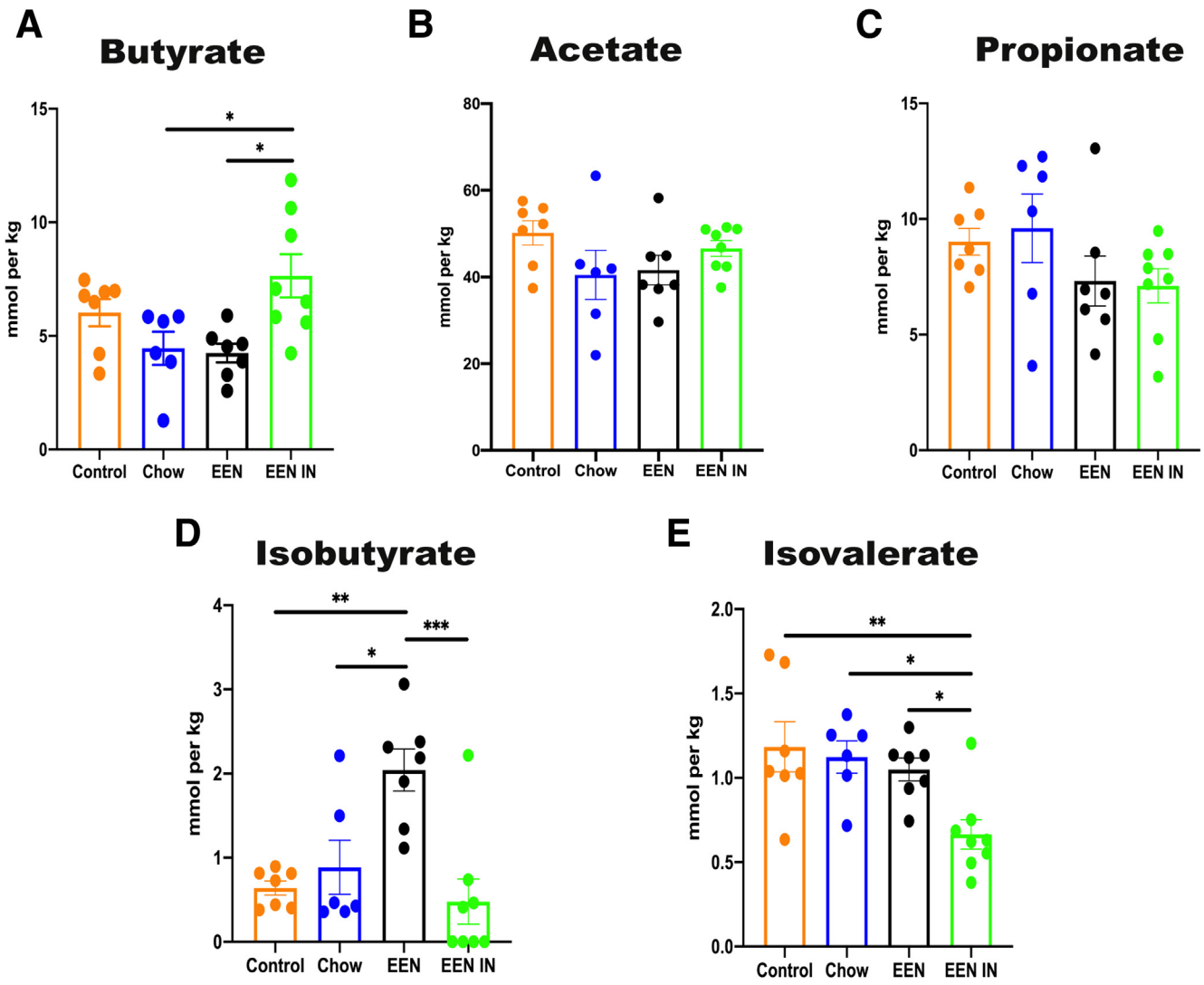

Figure 7. Concentration (mmoL/kg) differences between the 4 intervention groups for cecal levels of (*A*) butyrate, (*B*) acetate, (*C*) propionate, (*D*) isobutyrate, and (*E*) isovalerate. Data shown are mean ± standard error of the mean; n = 6–8 mice/group; each data point represents 1 mouse. Statistical analysis used one-way analysis of variance. *$P < .05$, **$P < .01$, ***$P < .001$.

EEN is considered one of the gold standard therapies used to treat newly diagnosed pediatric CD patients; therefore, we expected less severe colitis to develop in mice within the EEN group. However, the adoptive T-cell transfer model is more reflective of human UC (colonic involvement only) rather than CD; therefore, these results may align more closely with the lower EEN efficacy observed in UC patients.

Conclusion

We can conclude that within an adoptive T-cell transfer model of colitis, IN enriched EEN led to several favorable outcomes. EEN IN was superior to EEN and chow because it suppressed colitis development, resulted in less deterioration of the mucus layer, increased butyrate production, promoted increased relative abundance of beneficial microbes (*Bifidobacterium* spp. and *Anaerostipes caccae*), reduced relative abundance of potentially pathogenic microbes ([*Clostridium*] *innoccum* group spp. and *Escherichia-Shigella* spp.), and led to an expansion of anti-inflammatory T-cell subsets, including IL10 producing Foxp3^{+} Tregs. We postulate that the enhanced disease outcomes observed in EEN IN mice occurred via butyrate-dependent pathways that helped preserve the mucus layer and promoted an anti-inflammatory intestinal environment.

This study investigates whether the addition of IN to EEN leads to enhanced outcomes compared with fiber-free EEN, the predominant formula used as an induction therapy in pediatric CD. Novel alternative or complementary pediatric IBD therapies with minimal side effects are currently in high demand, particularly for pediatric UC patients, where to date nutritional interventions have provided minimal benefit in helping induce remission. These data provide preclinical evidence to support undertaking human studies to investigate whether IN enriched EEN is a

superior alternative option to fiber-free EEN for the treatment of both UC and CD patients.

Materials and Methods

Adoptive T-Cell Transfer Model of Colitis. TCR-$\beta^{-/-}$ C57BL/6 mice were bred at BC Children's Hospital Research Institute animal facility under specific pathogen-free conditions and were used at 8–14 weeks of age. A mix of both male and female mice were used, with a ratio of male to female of approximately 3:1 per group. We used 52 mice housed in at least 4 separate cages per group to help control for microbiome specific cage effects,[56] with 13 mice randomly assigned to each of the 4 intervention groups: (1) control group received a phosphate-buffered saline (PBS) intraperitoneal (IP) injection and standard chow diet (negative control), (2) chow group received a naive T-cell IP injection and standard chow diet (positive control), (3) EEN group received a naive T-cell IP injection and enteral formula without fiber, and (4) EEN IN group received a naive T-cell IP injection and enteral formula with fiber. Animal care, maintenance, and experimental procedures were approved by the University of British Columbia Animal Care Committee (permit number: A19-0254) and performed in accordance with the Canadian Council on Animal Care (CCAC).

Naive T-Cell Sorting and Adoptive T-Cell Transfer. Spleens and lymph nodes from female 8- to 12-week-old Thy1.1$^{+/+}$ Foxp3-eGFP mice[34] were processed into single cell suspensions by mashing the organs using a 40 μm nylon cell strainer. CD4$^+$ T cells were isolated from the cell suspension by magnetic bead selection (STEMCELL Technologies, Vancouver, Canada), then stained for viability (eFluor780; Thermo Fisher, Pittsburgh, PA), followed by surface staining using fluorescence conjugated anti-mouse CD4 (GK1.5, Thermo Fisher) and CD44 (IM7, Thermo Fisher). Naive CD4$^+$ T cells, defined as CD4$^+$, CD25^{neg}, CD44^{low}, and Foxp3$^{neg/low}$, were sorted by fluorescence activated cell sorting to a purity of 95%. The resulting naive CD4$^+$ T cells were washed twice with PBS, enumerated using a hemocytometer, and resuspended in PBS to a concentration of 2.5 million cells/mL.

A 200 μL aliquot of naive CD4$^+$ T cells (0.5 million cells) or PBS (control group only) were intraperitoneally injected into the recipient TCR-$\beta^{-/-}$ mice. This adoptive T-cell transfer leads to a gut microbiota dependent expansion of naive CD4$^+$ T cells into effector CD4$^+$ T cells, which leads to significant colitis by 4–8 weeks after injection.[57] Certain environmental factors (ie, diet) and/or changes in the gut microbiome have the potential to limit colitis development by promoting the expansion of anti-inflammatory CD4$^+$ T-cell subsets and suppressing pro-inflammatory CD4$^+$ T-cell subsets.

Diets. Mice were commenced on their respective diets immediately after naive CD4$^+$ T-cell adoptive transfer. The control and chow groups were provided with ad libitum access to water (H_2O) and to Teklad TD.97184 diet (Envigo, Madison, WI), a standard irradiated chow with 5% cellulose (poorly fermented fiber source). The EEN mice were fed ad libitum fiber-free enteral formula (Ensure Plus; Abbott Laboratories, Chicago, IL) in their H_2O bottles. The EEN IN mice were fed ad libitum enteral formula (Ensure Plus) enriched with 3% IN prebiotic (Orafti Synergy 1; Beneo, Mannheim, Germany) in their H_2O bottles (Table 1). The mice continued on their respective diets until the end of the experiment at 5 weeks after adoptive T-cell transfer.

Body Weight and Food Intake. Body weight and food intake were monitored daily. Change in body weight was reported as a percentage drop or gain in body weight from the original weight as measured on the day of adoptive T-cell transfer.

Disease Activity Scores. Disease activity was monitored in mice twice weekly until at least one mouse lost >10% body weight, and then disease activity was monitored daily. The DAS were determined using a previously reported scoring system,[58] which is based on percentage loss of body weight, stool consistency, and signs of intestinal bleeding.

Survival. If mice reached their humane endpoint before the end of the experiment, which was 5 weeks after adoptive T-cell transfer, they were euthanized. Humane endpoint was reached if mice lost >20% of their original body weight, had severe rectal excoriation due to diarrhea, and/or had a pronounced decline in activity with a hunched appearance.

Spleen Weight and Colon Length. At the end of the experiment, mice were anesthetized with isoflurane and then euthanized via carbon dioxide asphyxiation and cervical dislocation. Spleens were removed, weighed, and then stored on ice in PBS with 2% fetal bovine serum and 2 mmol/L EDTA before flow cytometry analysis. Colons were also removed, and their lengths were recorded. Each colon was then cut, and a longitudinal section of the distal colon was taken for H&E staining. A cross section of the mid-colon, which contained part of a fecal pellet to better visualize the mucus layer, was also taken for Alcian blue/periodic acid-Schiff (PAS) staining.

H&E and Alcian Blue/PAS Staining. The longitudinal distal colonic sections, used for H&E staining, were fixed in 10% neutral buffered formalin (Fischer Scientific) for 24 hours and then transferred to 70% ethanol. The cross sections of the mid colon, used for Alcian blue/PAS staining, were immediately fixed in methacarn (60% methanol, 10% acetic acid glacial, and 30% chloroform) at 4°C overnight and transferred to 100% methanol for 1 hour and then 100% ethanol. Fixed tissue was embedded in paraffin, and 4 μm sections were cut.

H&E Staining. H&E staining was performed using standard procedures. In brief, the slides were first washed in H_2O for 1 minute and then stained with hematoxylin for 5 minutes. The slides were washed again in H_2O for 1 minute and then dipped 1–2 times in 1% acid alcohol. After washing for 30 seconds the slides were added to saturated lithium carbonate for 30 seconds. The slides were washed again and then checked microscopically to ensure the nuclear staining was adequate. If necessary, the slides were re-stained by repeating the previous steps. The slides were next immersed in 70% isopropyl alcohol for 30 seconds and

then stained with 1% eosin (in 80% alcohol) for 15–30 seconds. The slides were added to 80% and then 90% isopropyl alcohol for 10 seconds each and then washed in 100% isopropyl alcohol twice for 1 minute each. They were allowed to air dry, and then a coverslip was added using mounting medium.

Histopathologic Scoring. H&E stained sections were blinded and imaged at ×20 magnification. Two blinded scorers used a modified version of a previously described histopathologic scoring system[59] to assess disease severity using 6 histopathologic criteria: (1) inflammatory cell infiltrate, (2) goblet cell loss, (3) crypt density loss, (4) crypt hyperplasia, (5) external muscle layer thickening, and (6) submucosal infiltration. The average of the scores of the 2 blinded scorers is reported.

Alcian Blue/PAS Staining. Slides were deparaffinized and rehydrated in distilled H_2O. The tissue sections were stained in Alcian blue 8GX (pH 2.5) for 30 minutes, and the slides were then washed in tap H_2O for 5 minutes. The slides were placed in periodic acid solution for 10 minutes and washed in tap water for an additional 5 minutes. The slides were then placed in Coleman's Schiff reagent solution for 10 minutes and washed in lukewarm distilled H_2O for 10 minutes. Last, the tissue sections were dehydrated using 95% ethanol, 100% ethanol, and xylene, each twice for 2 minutes, and the slides were mounted using resinous medium.

Mucus Layer Thickness and Goblet Cell Counting. Alcian blue/PAS stained sections were blinded and imaged at ×40 magnification. Between 7 and 10 images of each section of mid colonic tissue were taken. The mucus layer thickness and goblet cell numbers were evaluated using ImageJ (version 1.52q). For each image the average of 3 mucus layer thickness measurements and the average counts of goblet cells from 5 full-length, well-oriented crypts were obtained.

T-Cell Subset Analysis. Spleens and MLN were harvested from euthanized mice, processed into single cell suspensions, and stimulated with 50 ng/mL of phorbol 12-myristate 13-acetate (Sigma-Aldrich, St Louis, MO) and 1 μg of ionomycin (Sigma-Aldrich) for 4 hours in the presence of 1 μL/mL of Golgi-Plug (BD Biosciences, Franklin Lakes, NJ). After stimulation, cells were Fc-blocked with anti-CD16/32 antibody (93; BioLegend, San Diego, CA), viability stained (eFluor780; Thermo Fisher), and surface stained for anti-Thy1.1 (HIS51; Thermo Fisher), CD4 (GK1.5; Thermo Fisher), and CD25 (PC61; Thermo Fisher). After surface staining, cells were fixed with Fixation/Permeabilization buffer (Thermo Fisher) and intracellularly stained for the presence of T-bet (4B10; Thermo Fisher), Rorγt (AFKJS-9; Thermo Fisher), IL10 (JES5-16E3; Thermo Fisher), IL17A (eBio17B7; Thermo Fisher), IL22 (IL-22JOP; Thermo Fisher), interferon γ (XMG1.2; Thermo Fisher), and tumor necrosis factor (MP6-XT22; Thermo Fisher). Samples were analyzed on a 4-laser LSR II flow cytometer (BD Biosciences) and FlowJo software, version 10.7.1 (Tree Star, Ashland, OR).

Gut Microbiome Analysis. Stool samples were collected from mice the day of adoptive T-cell transfer (pre-intervention) as well as the day before the end of experiment (post-intervention). Cecal contents were collected at the end of the experiment for SCFA analysis. The stool and cecal samples were stored at −80°C until analysis.

DNA Extraction and Quantification. Bacterial genomic DNA was extracted from stool following the Omega E.N.Z.A Soil DNA kit instructions with a few minor modifications. In brief, 65 mg ± 5% of stool was weighed out into bead beating tubes. The stool was homogenized at 30 m/s for 3 minutes with bead beating solution. The DNA was eluted in 50 μL of elution buffer, and DNA concentrations were quantified using both a NanoDrop One (Thermo Fisher) spectrophotometer and Qubit 4 fluorometer (Thermo Fisher).

16S rRNA Library Preparation and Sequencing. Libraries were prepared and sequenced at the Sequencing and Bioinformatics Consortium at the University of British Columbia, Vancouver, BC, Canada. Briefly, the V3 and V4 regions of the 16S rRNA gene were polymerase chain reaction amplified using primers F: 5'-TCGTCGGCAGCGTCAGATGTGTATAAGAGACAGCCTACGGGN-GGCWGCAG and R: 5'-GTCTCGTGGGCTCGGAGATGTGTATAAGAGACAGGACTACHVGGGTATCTAATCC using 12.5 ng input DNA per sample. These were then converted to sequencing libraries using an 8-cycle indexing polymerase chain reaction with Nextera XT primers (Illumina, San Diego, CA). Libraries were then pooled and sequenced on a MiSeq (Illumina) to generate paired-end 250 base pair reads. Raw data were processed using bcl2fast v2.20.0.422 to generate demultiplexed fastq files.

Bioinformatic Analysis. Raw sequence data from the 16S rRNA hypervariable region V3-V4 was processed using a custom pipeline. Cutadapt (version 1.16)[60] was used to remove standard Illumina V3-V4 primers, and quality filtering was performed using the filterAndTrim function from the R package dada2 (version 1.18.0),[61] discarding forward and reverse reads with higher expected errors (EE = sum(10^(-Q/10)) than 3 and 5, respectively). A table of sequence variants was generated using the standard dada2 workflow, and taxonomic classifications were assigned to sequence variants using the Silva database, release 138.

An average of 49,239 reads was generated per sample. Preliminary analyses were carried out using the R package phyloseq (version 1.34.0).[62] Alpha diversity was estimated using species richness, and significance was determined using a Wilcoxon rank-sum test on the log10 difference between alpha diversity before intervention and after intervention. Beta diversity was estimated using a principal coordinates analysis on a matrix of Bray-Curtis distances. Before ordination, sequence variant counts were normalized using a variance-stabilizing transformation, and low abundance sequence variants were removed (those present in less than 5% of all samples). Statistical significance was determined using permutational multivariate analysis of variance.

Differential abundance analysis was carried out using DESeq2 (version 1.30.0)[63] to identify sequence variants that were differentially abundant within treatment groups between before intervention and after intervention. Variance-stabilizing transformation–normalized counts were modeled using the negative binomial distribution, and significance was determined by a Wald test on log2 fold change values and an alpha = 0.01. Significant differences in relative abundance between groups were determined using Kruskall-Wallis tests. *P* values were adjusted for multiple inference using the Benjamini-Hochberg method. Sequencing data are available from NCBI Sequence Read archive: http://www.ncbi.nlm.nih.gov/bioproject/731528.

SCFA Analysis Using Gas Chromatography. The SCFA extraction method used is identical to the procedure published by Zhao et al.[64] In brief, cecal samples were resuspended in MilliQ-grade H_2O and homogenized using MP Bio FastPrep for 1 minute at 4.0 m/s. Then 5 mol/L HCl was added to cecal suspensions to a final pH of 2.0. Acidified cecal suspensions were incubated and centrifuged at 10,000 rpm to separate the supernatant. Cecal supernatants were spiked with 2-ethylbutyric acid for a final concentration of 1 mmol/L. Extracted SCFA supernatants were stored in 2 mL GC vials with glass inserts. SCFAs were detected using gas chromatography (Thermo Trace 1310), coupled to a flame ionization detector (Thermo Fisher). The SCFA column used was the Thermo Fisher TG-WAXMS A GC column (30 m, 0.32 mm, 0.25 μm). The following settings were used for detection: flame ionization detector: temperature 240°C, hydrogen 35 mL/min, air 350 mL/min, makeup gas (nitrogen) 40 mL/min; inlet: carrier pressure 225 kPa, column flow 6 mL/min, purge flow 5 mL/min, split flow 12 mL/min, splitless time 0.75 minutes; oven: temperature gradient 100°–180°C, gradient time 10 minutes.

Statistical Analysis. One-way analysis of variance was used to determine whether there were any significant differences in T-cell subsets (only the chow, EEN, and EEN IN groups), spleen weight, colon length, body weight, DAS, SCFAs, goblet cell numbers, and mucus thickness between the 4 intervention groups. Two-way analysis of variance was used to determine whether there were any significant differences in histopathology scores between the 4 intervention groups. GraphPad Prism (San Diego, CA) software, version 8 for macOS, was used to perform all statistical analyses. All results presented are expressed as the mean values ± the standard errors of the mean. A *P* value of .05 or less was considered significant, with asterisks indicating significant differences in the figures. All authors had access to the study data and have reviewed and approved the final manuscript.

References

1. Abegunde AT, Muhammad BH, Bhatti O, Ali T. Environmental risk factors for inflammatory bowel diseases: evidence based literature review. World J Gastroenterol 2016;22:6296–6317.
2. Forbes A, Escher J, Hébuterne X, Klek S, Krznaric Z, Schneider S, Shamir R, Stardelova K, Wierdsma N, Wiskin AE, Bischoff SC. ESPEN guideline: clinical nutrition in inflammatory bowel disease. Clin Nutr 2017;36:321–347.
3. Ruemmele F, Veres G, Kolho K, Griffiths A, Levine A, Escher JC, Amil Dias J, Barabino A, Braegger CP, Bronsky J, Buderus S, Martin-de-Carpi J, De Ridder L, Fagerberg UL, Hugot JP, Kierkus J, Kolacek S, Koletzko S, Lionetti P, Miele E, Navas Lopez VM, Paerregaard A, Russell RK, Serban DE, Shaoul R, Van Rheenen P, Veres Veereman G, Weiss B, Wilson D, Dignass A, Eliakim A, Winter H, Turner D. Consensus guidelines of ECCO/ESPGHAN on the medical management of pediatric Crohn's disease. J Crohns Colitis 2014;8:1179–1207.
4. Berni Canani R, Terrin G, Borrelli O, Romano MT, Manguso F, Coruzzo A, D'Armiento F, Romeo EF, Cucchiara S. Short- and long-term therapeutic efficacy of nutritional therapy and corticosteroids in paediatric Crohn's disease. Dig Liver Dis 2006;38:381–387.
5. MacLellan A, Connors J, Grant S, Cahill L, Langille MGI, Van Limbergen J. The impact of exclusive enteral nutrition (EEN) on the gut microbiome in Crohn's disease: a review. Nutrients 2017;9:1–14.
6. Papada E, Kaliora AC, Gioxari A, Papalois A, Forbes A. Anti-inflammatory effect of elemental diets with different fat composition in experimental colitis. Br J Nutr 2014;111:1213–1220.
7. Alhagamhmad MH, Lemberg DA, Day AS, Tan LZ, Ooi CY, Krishnan U, Gupta N, Munday JS, Leach ST. Advancing nutritional therapy: a novel polymeric formulation attenuates intestinal inflammation in a murine colitis model and suppresses pro-inflammatory cytokine production in ex-vivo cultured inflamed colonic biopsies. Clin Nutr 2017;36:497–505.
8. Nahidi L, Leach ST, Mitchell HM, Kaakoush NO, Lemberg DA, Munday JS, Huinao Karina, Day AS. Inflammatory bowel disease therapies and gut function in a colitis mouse model. Biomed Res Int 2013;2013:1–15.
9. Hill RJ. Nutritional support and dietary interventions for patients with ulcerative colitis: current insights. Nutr Diet Suppl 2016;8:41–49.
10. Assa A, Shamir R. Exclusive enteral nutrition for inducing remission in inflammatory bowel disease in paediatric patients. Curr Opin Clin Nutr Metab Care 2017;20:384–389.
11. Lewis JD, Chen EZ, Baldassano RN, Otley AR, Griffiths AM, Lee D, Bittinger K, Bailey A, Friedman ES, Hoffmann C, Albenberg L, Sinha R, Compher C, Gilroy E, Nessel L, Grant A, Chehoud C, Li Hongzhe, Wu GD, Bushman FD. Inflammation, antibiotics, and diet as environmental stressors of the gut microbiome in pediatric Crohn's disease. Cell Host Microbe 2015;18:489–500.
12. Quince C, Ijaz UZ, Loman N, Eren AM, Saulnier D, Russell J, Haig SJ, Calus ST, Quick J, Barclay A, Bertz M, Blaut M, Hansen R, Mcgrogan P, Russell RK, Edwards CA, Gerasimidis K. Extensive modulation of the fecal metagenome in children with Crohn's disease

during exclusive enteral nutrition. Am J Gastroenterol 2015;110:1718–1729.
13. Dunn KA, Moore-Connors J, Macintyre B, Stadnyk AW, Thomas NA, Noble A, Mahdi G, Rashid M, Otley AR, Bielawski JP, Van Limbergen J. Early changes in microbial community structure are associated with sustained remission after nutritional treatment of pediatric Crohn's disease. Inflamm Bowel Dis 2016;22:2853–2862.
14. Ishikawa H, Matsumoto S, Ohashi Y, Imaoka A, Setoyama H, Umesaki Y, Tanaka R, Otani T. Beneficial effects of probiotic Bifidobacterium and galactooligosaccharide in patients with ulcerative colitis: a randomized controlled study. Digestion 2011;84:128–133.
15. Lindsay JO, Whelan K, Stagg AJ, Gobin P, Al-Hassi HO, Rayment N, Kamm MA, Knight SC, Forbes A. Clinical, microbiological, and immunological effects of fructooligosaccharide in patients with Crohn's disease. Gut 2006;55:348–356.
16. Healey GR, Celiberto LS, Lee SM, Jacobson K. Fiber and prebiotic interventions in pediatric inflammatory bowel disease: what role does the gut microbiome play? Nutrients 2020;12.
17. Joossens M, Huys G, Cnockaert M, De Preter V, Verbeke K, Rutgeerts P, Vandamme P, Vermeire S. Dysbiosis of the faecal microbiota in patients with Crohn's disease and their unaffected relatives. Gut 2011;60:631–637.
18. Burton-Freeman B. Dietary fiber and energy regulation. J Nutr 2000;130:272–275.
19. Guarner F. Inulin and oligofructose impact on intestinal diseases and disorders. Br J Nutr 2005;93:S61–S65.
20. Fernandes R, do Rosario VA, Mocellin MC, Kuntz MGF, Trindade EBSM. Effects of inulin-type fructans, galactooligosaccharides and related synbiotics on inflammatory markers in adult patients with overweight or obesity: a systematic review. Clin Nutr 2017;36:1197–1206.
21. Swanson KS, de Vos WM, Martens EC, Gilbert JA, Menon RS, Soto-Vaca A, Hautvast J, Meyer PD, Borewicz K, Vaughan EE, Slavin JL. Effect of fructans, prebiotics and fibres on the human gut microbiome assessed by 16S rRNA-based approaches: a review. Benef Microbes 2020;11:101–129.
22. Schwiertz A, Hold GL, Duncan SH, Gruhl B, Collins MD, Lawson PA, Flint HJ, Blaut M. Anaerostipes caccae gen. nov., sp. nov., a new saccharolytic, acetate-utilising, butyrate-producing bacterium from human faeces. Syst Appl Microbiol 2002;25:46–51.
23. Louis P, Flint HJ. Formation of propionate and butyrate by the human colonic microbiota. Environ Microbiol 2017;19:29–41.
24. Wu X, Wu Y, He L, Wu L, Wang X, Liu Z. Effects of the intestinal microbial metabolite butyrate on the development of colorectal cancer. J Cancer 2018;9:2510–2517.
25. Gao Z, Yin J, Zhang J, Ward RE, Martin RJ, Lefevre M, Cefalu WT, Ye J. Butyrate improves insulin sensitivity and increases energy expenditure in mice. Diabetes 2009;58:1509–1517.
26. Segain JP, Galmiche JP, Raingeard De La Blétière D, Bourreille A, Leray V, Gervois N, Rosales C, Ferrier L, Bonnet C, Blottière HM. Butyrate inhibits inflammatory responses through NFκB inhibition: implications for Crohn's disease. Gut 2000;47:397–403.
27. Lin HV, Frassetto A, Kowalik EJ, Nawrocki AR, Lu MM, Kosinski JR, Hubert JA, Szeto D, Yao X, Forrest G, Marsh DJ. Butyrate and propionate protect against diet-induced obesity and regulate gut hormones via free fatty acid receptor 3-independent mechanisms. PLoS One 2012;7:1–9.
28. Peng L, Li ZR, Green RS, Holzman IR, Lin J. Butyrate enhances the intestinal barrier by facilitating tight junction assembly via activation of AMP-activated protein kinase in Caco-2 cell monolayers. J Nutr 2009;139:1619–1625.
29. Furusawa Y, Obata Y, Fukuda S, Endo T, Nakato G, Takahashi D, Nakanishi Y, Uetake C, Kato K, Kato T, Takahashi M, Fukuda NN, Murakami S, Miyauchi Eiji, Hino S, Atarashi K, Onawa S, Fujimura Y, Lockett T, Clarke JM, Topping DL, Tomita M, Hori S, Ohara O, Morita T, Koseki H, Kikuchi Jun, Honda K, Hase K, Ohno H. Commensal microbe-derived butyrate induces the differentiation of colonic regulatory T cells. Nature 2013;504:446–450.
30. Zhang Z, Zhou X. Foxp3 instability helps Tregs distinguish self and non-self. Front Immunol 2019;10:1–6.
31. Whibley N, Tucci A, Powrie F. Regulatory T cell adaptation in the intestine and skin. Nat Immunol 2019;20:386–396.
32. Pandiyan P, Bhaskaran N, Zou M, Schneider E, Jayaraman S, Huehn J. Microbiome dependent regulation of Tregs and Th17 cells in mucosa. Front Immunol 2019;10:1–17.
33. Noval Rivas M, Chatila TA. Regulatory T cells in allergic diseases. J Allergy Clin Immunol 2016;138:639–652.
34. Yao Y, Vent-Schmidt J, McGeough MD, Wong M, Hoffman HM, Steiner TS, Levings MK. Tr1 cells, but not Foxp3 + regulatory T cells, suppress NLRP3 inflammasome activation via an IL-10–dependent mechanism. J Immunol 2015;195:488–497.
35. Choi JM, Bothwell ALM. The nuclear receptor PPARs as important regulators of T-cell functions and autoimmune diseases. Mol Cells 2012;33:217–222.
36. Bassaganya-Riera J, DiGuardo M, Viladomiu M, de Horna A, Sanchez S, Einerhand AWC, Sanders L, Hontecillas R. Soluble fibers and resistant starch ameliorate disease activity in interleukin-10-deficient mice with inflammatory bowel disease. J Nutr 2011;141:1318–1325.
37. Park J, Wang Q, Wu Q, Mao-Draayer Y, Kim CH. Bidirectional regulatory potentials of short-chain fatty acids and their G-protein-coupled receptors in autoimmune neuroinflammation. Sci Rep 2019;9:1–13.
38. Arpaia N, Campbell C, Fan X, Dikiy S, Van Der Veeken J, Deroos P, Liu H, Cross JR, Pfeffer K, Coffer PJ, Rudensky AY. Metabolites produced by commensal bacteria promote peripheral regulatory T-cell generation. Nature 2013;504:451–455.
39. Yang W, Yu T, Huang X, Bilotta AJ, Xu L, Lu Y, Sun J, Pan F, Zhou J, Zhang W, Yao S, Maynard CL,

Singh N, Dann SM, Liu Z, Cong Y. Intestinal microbiota-derived short-chain fatty acids regulation of immune cell IL-22 production and gut immunity. Nat Commun 2020:11.

40. Lo BC, Shin SB, Canals Hernaez D, Refaeli I, Yu HB, Goebeler V, Cait A, Mohn WW, Vallance BA, McNagny KM. IL-22 preserves gut epithelial integrity and promotes disease remission during chronic salmonella infection. J Immunol 2019;202:956–965.
41. Cook L, Stahl M, Han X, Nazli A, MacDonald KN, Wong MQ, Tsai K, Dizzell S, Jacobson K, Bressler B, Kaushic C, Vallance BA, Steiner TS, Levings MK. Suppressive and gut-reparative functions of human type 1 T regulatory cells. Gastroenterology 2019;157:1584–1598.
42. Busbee PB, Alrafas H, Dopkins N, Nagarkatti M, Nagarkatti PS. Indole-3-carbinol prevents murine colitis development via an IL-22-dependent mechanism that regulates anti- microbial peptides and mucus production. J Immunol 2019;202:12–19.
43. Jung TH, Park JH, Jeon WM, Han KS. Butyrate modulates bacterial adherence on LS174T human colorectal cells by stimulating mucin secretion and MAPK signaling pathway. Nutr Res Pract 2015;9:343–349.
44. Desai MS, Seekatz AM, Koropatkin NM, Kamada N, Hickey CA, Wolter M, Pudlo NA, Kitamoto S, Terrapon N, Muller A, Young VB, Henrissat B, Wilmes P, Stappenbeck TS, Núñez G, Martens EC. A dietary fiber-deprived gut microbiota degrades the colonic mucus barrier and enhances pathogen susceptibility. Cell 2016; 167:1339–1353.e21.
45. Schroeder BO, Birchenough GMH, Ståhlman M, Arike L, Johansson MEV, Hansson GC, Bäckhed F. Bifidobacteria or fiber protects against diet-induced microbiota-mediated colonic mucus deterioration. Cell Host Microbe 2018;23:27–40.e7.
46. Matt SM, Allen JM, Lawson MA, Mailing LJ, Woods JA, Johnson RW. Butyrate and dietary soluble fiber improve neuroinflammation associated with aging in mice. Front Immunol 2018;9.
47. Pittayanon R, Lau JT, Yuan Y, Leontiadis GI, Tse F, Surette M, Moayyedi P. Gut microbiota in patients with irritable bowel syndrome: a systematic review. Gastroenterology 2019;157:97–108.
48. Le Chatelier E, Nielsen T, Qin J, Prifti E, Hildebrand F, Falony G, Almeida M, Arumugam M, Batto J, Kennedy S, Leonard P, Li J, Burgdorf K, Grarup N, Jørgensen T, Brandslund I, Nielsen HB, Juncker AS, Bertalan M, Levenez F, Pons N, Rasmussen S, Sunagawa S, Tap J, Tims S, Zoetendal EG, Brunak Søren, Clément K, Doré J, Kleerebezem M, Kristiansen K, Renault P, Sicheritz-Ponten T, de Vos WM, Zucker J, Raes J, Hansen T, Bork P, Wang J, Ehrlich SD, Pedersen O. Richness of human gut microbiome correlates with metabolic markers. Nature 2013;500:541–546.
49. Glassner KL, Abraham BP, Quigley EMM. The microbiome and inflammatory bowel disease. J Allergy Clin Immunol 2020;145:16–27.
50. Gatti S, Galeazzi T, Franceschini E, Annibali R, Albano V, Verma A, De Angelis M, Lionetti M, Catassi C. Effects of the exclusive enteral nutrition on the microbiota profile of patients with Crohn's disease: a systematic review. Nutrients 2017;9:1–14.
51. Hung YP, Lin HJ, Wu CJ, Chen PL, Lee JC, Liu HC, Wu YH, Yeh FH, Tsai PJ, Ko WCh. Vancomycin-resistant Clostridium innocuum bacteremia following oral vancomycin for Clostridium difficile infection. Anaerobe 2014; 30:24–26.
52. Ackermann G, Tang YJ, Jang SS, Silva JJ, Rodloff AC, Cohen SH. Isolation of Clostridium innocuum from cases of recurrent diarrhea in patients with prior Clostridium difficile associated diarrhea. Diagn Microbiol Infect Dis 2001;40:103–106.
53. Singh S, Bhatia R, Khare P, Sharma S, Rajarammohan S, Bishnoi M, Bhadada SK, Sharma SS, Kaur J, Kondepudi KK. Anti-inflammatory Bifidobacterium strains prevent dextran sodium sulfate induced colitis and associated gut microbial dysbiosis in mice. Sci Rep 2020;10:1–14.
54. Deehan EC, Yang C, Perez-Muñoz ME, Nguyen NK, Cheng CC, Triador L, Zhang Z, Bakal JA, Walter J. Precision microbiome modulation with discrete dietary fiber structures directs short-chain fatty acid production. Cell Host Microbe 2020;27:389–404.e6.
55. Windey K, de Preter V, Verbeke K. Relevance of protein fermentation to gut health. Mol Nutr Food Res 2012; 56:184–196.
56. Hildebrand F, Nguyen TLA, Brinkman B, Yunta RG, Cauwe B, Vandenabeele P, Liston A, Raes J. Inflammation-associated enterotypes, host genotype, cage and inter-individual effects drive gut microbiota variation in common laboratory mice. Genome Biol 2013; 14:1–15.
57. Eri R, McGuckin MA, Wadley R. T cell transfer model of colitis: a great tool to assess the contribution of T cells in chronic intestinal inflammation. Methods Mol Biol 2012; 844:261–271.
58. Wirtz S, Popp V, Kindermann M, Gerlach K, Weigmann B, Fichtner-Feigl S, Neurath MF. Chemically induced mouse models of acute and chronic intestinal inflammation. Nat Protoc 2017;12:1295–1309.
59. Koelink PJ, Wildenberg ME, Stitt LW, Feagan BG, Koldijk M, van Wout AB, Atreya R, Vieth M, Brandse JF, Duijst S, te Velde AA, D'Haens GRAM, Levesque BG, van den Brink GR. Development of reliable, valid and responsive scoring systems for endoscopy and histology in animal models for inflammatory bowel disease. J Crohns Colitis 2018;12:794–803.
60. Martin M. Cutadapt removes adapter sequences from high-throughput sequencing reads. EMBnetJournal 2011;17:10–12.
61. Callahan BJ, McMurdie PJ, Rosen MJ, Han AW, Johnson AJA, Holmes SP. DADA2: high-resolution sample inference from Illumina amplicon data. Nat Methods 2016;13:581–583.
62. McMurdie PJ, Holmes S. Phyloseq: an R package for reproducible interactive analysis and graphics of microbiome census data. PLoS One 2013;8.

63. Love MI, Huber W, Anders S. Moderated estimation of fold change and dispersion for RNA-seq data with DESeq2. Genome Biol 2014;15:1–21.
64. Zhao G, Nyman M, Jonsson JA. Rapid determination of short-chain fatty acids in colonic contents and faeces of humans and rats by acidified water-extraction and direct-injection gas chromatography. Biomed Chromatogr 2006;20:674–682.

Received December 15, 2020. Accepted June 16, 2021.

Correspondence
Address correspondence to: Bruce A. Vallance, BC Children's Hospital Research Institute, University of British Columbia, Vancouver, Canada. Phone: (604) 875-2345 ext 5112. e-mail: bvallance@cw.bc.ca; or Kevan Jacobson, MBBCh, BC Children's Hospital Research Institute, University of British Columbia, Vancouver, Canada. Phone: (604) 875-2332 ext 1. e-mail: kjacobson@cw.bc.ca.

CRediT Authorship Contributions
Genelle R. Healey (Conceptualization: Equal; Data curation: Lead; Formal analysis: Lead; Investigation: Lead; Methodology: Equal; Project administration: Lead; Validation: Lead; Visualization: Lead; Writing – original draft: Lead; Writing – review & editing: Equal)

Kevin Tsai (Conceptualization: Supporting; Formal analysis: Supporting; Investigation: Supporting; Methodology: Supporting; Validation: Supporting; Writing – original draft: Supporting; Writing – review & editing: Supporting)

Alana Schick (Conceptualization: Supporting; Formal analysis: Supporting; Methodology: Supporting; Writing – review & editing: Supporting)

Daniel J. Lisko (Conceptualization: Supporting; Investigation: Supporting; Methodology: Supporting; Writing – original draft: Supporting; Writing – review & editing: Supporting)

Laura Cook (Conceptualization: Supporting; Formal analysis: Supporting; Methodology: Supporting; Writing – review & editing: Supporting)

Bruce A. Vallance (Conceptualization: Supporting; Funding acquisition: Equal; Methodology: Equal; Supervision: Equal; Writing – original draft: Supporting; Writing – review & editing: Supporting)

Kevan Jacobson, MBBCh, FRCP(C), FCP (Conceptualization: Equal; Funding acquisition: Equal; Methodology: Equal; Supervision: Equal; Writing – original draft: Supporting; Writing – review & editing: Supporting)

Conflicts of interest
The authors disclose no conflicts.

Funding
Supported by discovery grants (2016-05338 [KJ], 2018-05120 [BAV]) from the Natural Sciences and Engineering Research Council, the Children with Intestinal and Liver Disorders (CHILD) Foundation (KJ), operating grants (PJT-148846 and 159528 [BAV]) from the Canadian Institutes of Health Research (CIHR) and Crohn's and Colitis Canada, and a Trainee Award from the Michael Smith Foundation for Health Research (17829 [GRH]).